

Ultra-low Hysteresis in Giant Magnetocaloric $\text{Mn}_{1-x}\text{V}_x\text{Fe}(\text{P}, \text{Si}, \text{B})$ Compounds

Jiawei Lai^{1,2*}, Bowei Huang^{1,2}, Dimitrios Bessas,² Xinmin You², Michael Maschek²,

Dechang Zeng^{1*}, L. Zhang², Niels van Dijk², Ekkes Brück²

*1. School of Materials Science & Engineering, South China University of Technology, Guangzhou
510640, China;*

*2. Fundamental Aspects of Materials and Energy, Department of Radiation Science and
Technology, TU Delft, Mekelweg 15, 2629JB Delft, The Netherlands*

Abstract

Large thermal hysteresis in the $\text{MnFe}(\text{P}, \text{Si}, \text{B})$ system hinders the heat exchange rate and thus limits the magnetocaloric applications at high frequencies. Substitution of Mn by V in $\text{Mn}_{1-x}\text{V}_x\text{Fe}_{0.95}\text{P}_{0.593}\text{Si}_{0.33}\text{B}_{0.077}$ and $\text{Mn}_{1-x}\text{V}_x\text{Fe}_{0.95}\text{P}_{0.563}\text{Si}_{0.36}\text{B}_{0.077}$ alloys was found to reduce the thermal hysteresis due to a decrease in the latent heat. Introducing V increases both the field-induced transition temperature shift and the magnetic moment per formula unit. Thus, a decrease in the thermal hysteresis is obtained without losing the giant magnetocaloric effect. In consequence, an ultralow hysteresis (0.7 K) and a giant adiabatic temperature change of 2.3 K were achieved, which makes these alloys promising candidates for commercial magnetic refrigerator using permanent magnets.

Keywords: $(\text{Mn}, \text{V}, \text{Fe})_{1.95}(\text{P}, \text{Si}, \text{B})$; Magnetocaloric; Magnetic properties; Entropy.

1. Introduction

Room temperature magnetic refrigeration technology has attracted broad attention due to its advantages compared to the traditional cooling techniques, such as a high efficiency and a low impact on the environment. ^[1] Materials with a giant magnetocaloric effect (GMCE), which are the working refrigerant of this technique, will release heat when an external magnetic field is applied, while they absorb heat when the magnetic field is removed. The performance of GMCE materials mainly determine the working efficiency and the cooling power of this technology. The GMCE usually occurs in materials that show a first-order magnetic transition (FOMT), such as $\text{Gd}_5\text{Ge}_2\text{Si}_2$, ^[2] $\text{LaFe}_{13-x}\text{Si}_x$, ^[3,4,5] $\text{MnFeP}_{1-x}\text{As}_x$, ^[6] $\text{MnFeP}_{1-x-y}\text{Si}_x\text{B}_y$, ^[7,8,9] MnCoGeB_x ^[10] and Heusler ^[11] alloys. Among them, the $\text{MnFeP}_{1-x-y}\text{Si}_x\text{B}_y$ alloys are regarded as one of the most promising materials that can be industrialized as magnetic refrigerant because of their cheap and non-toxic elements, high cooling capacity and tunable T_C near room temperature. ^[7]

Thermal hysteresis (ΔT_{hys}) is an important issue that limits the real application of the GMCE in these FOMT materials. ^[12] The discontinuous nature of the transition is the feature that provides the GMCE. Therefore, in the premise of keeping the GMCE, the thermal hysteresis should be made as narrower as possible by manipulating the microstructure or by tuning the composition. Through 0.075 at.% of B substitution in the $\text{MnFeP}_{1-x-y}\text{Si}_x\text{B}_y$ alloys, the optimized ΔT_{hys} can be decreased to 1.6 K according to temperature-dependent magnetization curves at a magnetic field of 1 T and ΔT_{hys} is 2.0 K according to in-field DSC measurements at a magnetic field of 1 T (see the supporting information of ref [9]), while maintaining a GMCE. ^[9] In this case, the material can be cycled for 10 thousand times and the sample geometry remains intact. A higher level of B substitution can decrease the ΔT_{hys} further, but

fail to provide a sufficiently large GMCE.^[13] It is essential to find a new approach to further decrease the ΔT_{hys} and simultaneously provide a large GMCE. One of the design criteria is that the adiabatic temperature change (ΔT_{ad}) should be larger than 2 K^[14], since Engelbrecht and Bahl^[15] demonstrated that cooling may be ineffective when ΔT_{ad} drops below 2 K. In this work, through V substitution, an ultra-low ΔT_{hys} (0.7 K) and a GMCE of ΔT_{ad} (2.3 K) at a magnetic field of 1 T is achieved simultaneously.

The crystal structure of $MnFeP_{1-x-y}Si_xB_y$ shows a significant change in lattice parameters across the magnetic phase transition, while it keeps its hexagonal structure (magneto-elastic transition).^[16,9] Applying a magnetic field results in a shift of the transition temperature (T_c) to higher temperatures. The shift of T_c induced by magnetic fields, defined as dT_c/dB , is positive for a conventional first-order magnetic transition materials such as $MnFeP_{1-x-y}Si_xB_y$ ^[13] and La-Fe-Si^[17], while it is negative for the inverse first-order magnetic transition materials, for instance the Ni-Mn-X-Heusler alloys with X = Sn, Sb and In^[18] or Fe-Rh^[19]. For the conventional first-order magnetic transition materials, this shift is attributed to the magnetic field stabilization of the phase with the higher magnetization, being the low-temperature ferromagnetic phase^[20,21]. In a magnetic field thermal energy is then needed to induce the magnetic phase transition. If the value of dT_c/dB is enhanced, the magnetic phase transition can be induced in lower magnetic field. As a consequence, low-field permanent magnets could be utilized, which would significantly reduce the costs of commercial applications. The magnetic field currently used in the commercial prototypes is generated by NdFeB permanent magnets with external magnetic fields varying from an 0.9 to 1.5 T^[22,23,24]. The materials cost to reach a field of 1.5 T may be 10 times higher than the costs to reach a field of 0.9 T. It is therefore of interest to explore the lower field potential of this GMCE system by studying

dT/dB . In this work, we investigated the effect of V substitution on the ΔT_{hys} , dT/dB , the lattice parameters and the magnetic properties in polycrystalline Mn-V-Fe-P-Si-B alloys.

2. Experimental

Polycrystalline $Mn_{1-x}V_xFe_{0.95}P_{0.593}Si_{0.33}B_{0.077}$ ($x = 0.00, 0.01, 0.02, 0.03$) alloys were prepared by a powder metallurgy method. The starting materials in the form of Mn, Fe, red P, Si and V powders were mechanically ball milled for 10 h in an Ar atmosphere with a constant rotation speed of 380 rpm, then pressed into small tablets, and finally sealed in quartz ampoules under 200 mbar of Ar before employing the various heat treatment conditions. These tablets were annealed at 1323 K for 2 h in order to crystalize and slowly cooled down to room temperature. Then they were heated up to the same annealing temperature for 20 h to homogenize the alloy and finally quenched in water. This batch samples is regarded as *series A*. In order to tune the T_C to room temperature for the sample with V, the $Mn_{1-x}V_xFe_{0.95}P_{0.563}Si_{0.36}B_{0.077}$ ($x = 0.00, 0.01, 0.02, 0.03$) alloys with a higher Si content were prepared with the same procedure as series A, except for a higher annealing temperature of 1373 K. This batch samples is regarded as *series B*.

The X-ray diffraction (XRD) patterns were collected on a PANalytical X-pert Pro diffractometer with Cu-K α radiation (1.54056 Å) at room temperature. The temperature and magnetic field dependence of the magnetization was measured with a commercial superconducting quantum interference device (SQUID) magnetometer (Quantum Design MPMS 5XL) in the reciprocating sample option (RSO) mode. The adiabatic temperature change (ΔT_{ad}) is measured in a Peltier cell based differential scanning calorimetry using a

Halbach cylinder providing a magnetic field of 1.5 T. In this setup, the iso-field calorimetric scans were performed at a slow rate of 50 mKmin⁻¹ in order to probe the equilibrium state, while the temperature has been corrected for the effect of the thermal resistance of the Peltier cells.

3. Results and discussions

In figure 1 the XRD patterns for *series A* (Fig. 1a and 1b) and *series B* (Fig. 1c and 1d) are illustrated. For the Mn_{1-x}V_xFe_{0.95}P_{0.563}Si_{0.36}B_{0.077} ($x = 0.00, 0.01$) alloys in *series B*, as T_C is higher than room temperature, the XRD patterns are measured at 323 K, where they are in the paramagnetic state. Other samples are measured at room temperature since their T_C values are below room temperature. At the selected temperatures, all the samples are measured at paramagnetic state. The hexagonal Fe₂P-type (space group P-62m) phase is identified as the main phase in all these alloys and the cubic MnFe₂Si-type phase (space group Fm3m) is identified as the impurity phase. Based on the refinement results, the estimated fraction of the impurity phase is 1.6 - 2.4 vol.% in *series A* and 3.7 - 4.5 vol.% in the *series B*, respectively. The amount of impurity phase is decreases by V substitution for *series B*. The lattice parameter in *series A* and *series B* shows a different behavior. For *series A*, an increase in V substitution leads to a decrease in the a axis and an increase in the c axis. The c/a ratio increases, while T_C decreases for an increasing V substitution. Note that, the unit cell volume of the crystal remains unchanged for $x = 0.01$ and 0.02. Only when the V content reaches $x = 0.03$, the volume drops by 0.7% compared to $x = 0.00$. For *series B*, the lattice parameters show a different trend. Oppositely, an increasing V substitution leads to an increase in the a axis, while the c axis decreases for $x = 0.00, 0.01$ and 0.02. The evolution of the unit cell volume for *series B* was found to differ from *series A* as the unit cell volume slightly

increases for $x = 0.02$ and 0.03 , but still smaller than $x = 0.00$. Since the covalent radius of V (132 ± 5 pm) is slightly smaller than that of Mn (139 ± 5 pm), a decrease in the unit cell volume may be a sign of the substitution of Mn by V in the Fe_2P -type structure.

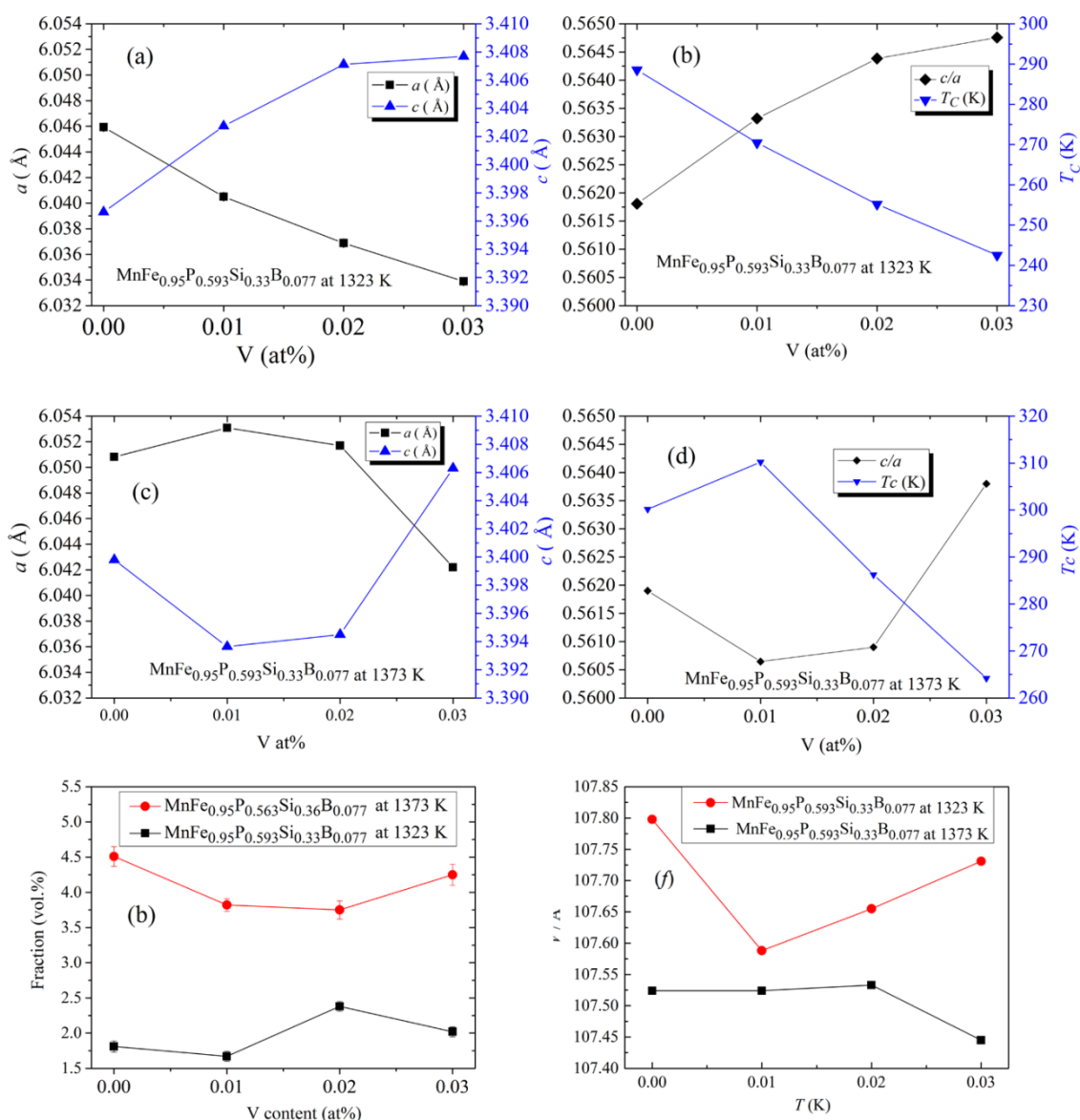


Fig. 1 (a) Lattice parameters of the a and c axis for series A and (b) c/a ratio and T_C for series A; (c) Lattice parameters of the a and c axis for series B and (d) c/a ratio and T_C for series B; (e) Fraction of the second phase in series A and B; (f) Unit cell volume of series A and B.

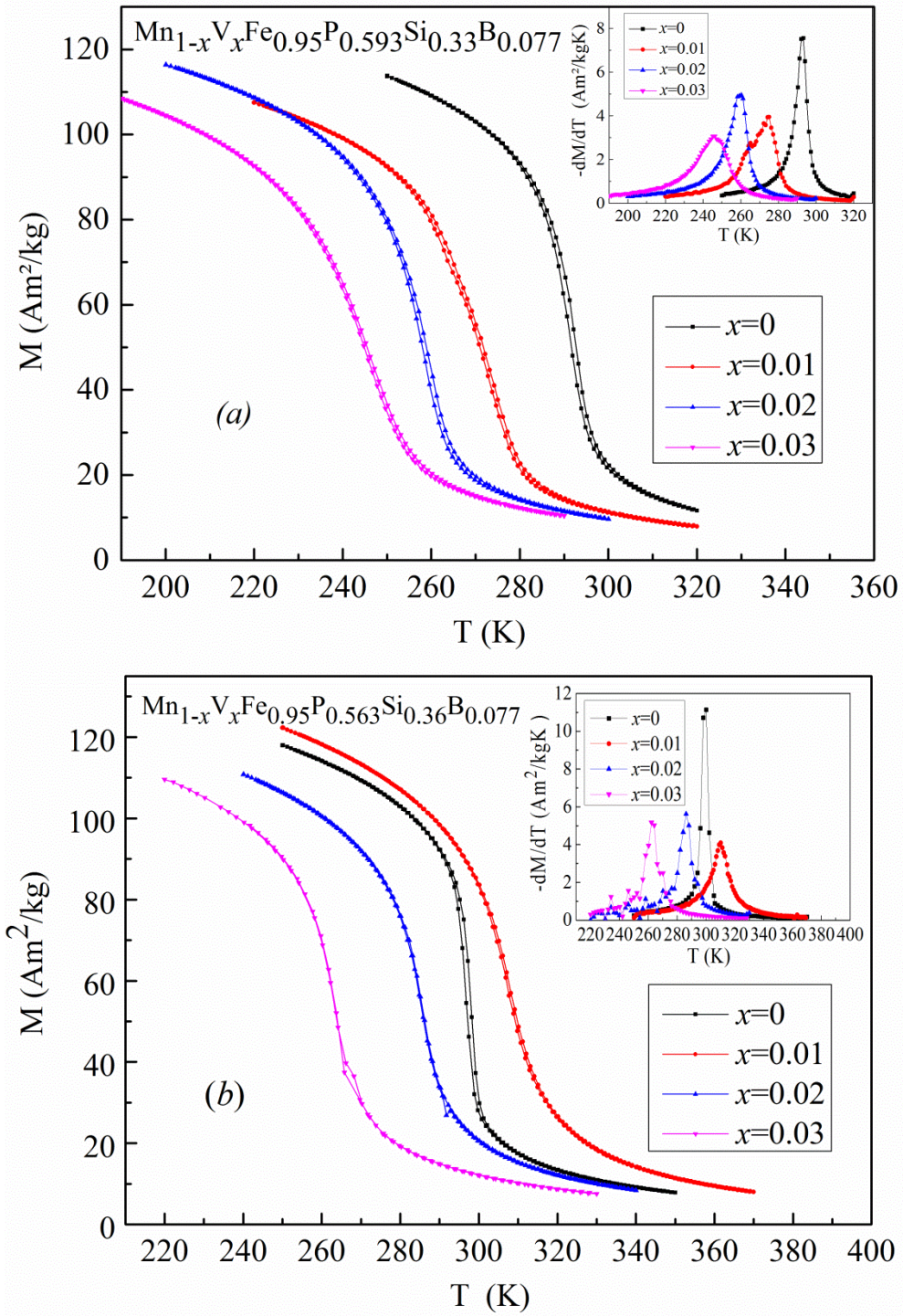


Fig. 2 (a) Temperature dependence of the magnetization in *series A* under an applied magnetic field of 1 T; (b) Temperature dependence of the magnetization in *series B* under an applied magnetic field of 1 T.

Table 1 The Curie temperature (T_C), thermal hysteresis (ΔT_{hys-MT}), latent heat (L), magnetic entropy change ($|\Delta S_M|$) and adiabatic temperature change ΔT_{ad} at a field change of 1 T for *series A* and *B*.

Annealed T (K)	Sample	T_C (K)	ΔT_{hys-MT} (K)	L (kJ/kg)	$ \Delta S_M $ (J/(kg·K))	ΔT_{ad} (K)
<i>series A</i>	$x = 0.00$	290.0	1.1	5.2	6.5	2.7
<i>series A</i>	$x = 0.01$	270.4	0.8	3.4	3.3	/
<i>series A</i>	$x = 0.02$	255.2	0.9	2.4	4.6	1.6
<i>series A</i>	$x = 0.03$	242.5	0.7	1.7	2.7	/
<i>series B</i>	$x = 0.00$	300.2	1.5	6.2	11.3	3.5
<i>series B</i>	$x = 0.01$	310.2	0.8	2.5	4.8	1.8
<i>series B</i>	$x = 0.02$	286.2	0.5	3.7	5.6	2.3
<i>series B</i>	$x = 0.03$	264.2	0.1	2.8	4.8	1.6
Ref. [9]*	$x = 0.00$	281	1.6	3.8	9.8	2.5

Temperature dependence of the magnetization in *series A* and *B* are shown in figure 2 (a) and (b), respectively. The temperature dependence of $-dM/dT$ is also shown in the corresponding insets. Generally, the maximum of $-dM/dT$ is regarded an indication of the strength for FOMT. The maximum of $-dM/dT$ in our materials decreases for an increasing V content except for the sample with $x = 0.02$, indicating it moves closer to SOMT. The reason why the sample with $x = 0.02$ has this jump is unclear. The transition temperature T_C is determined from the maximum value of the $-dM/dT$ in the $M-T$ curve during heating. For *series A*, T_C tends to decrease with increasing V substitution. Moreover, the reduction of T_C becomes weaker with increasing V content, as shown in table 1. It reduces from about 18.1, 15.3 and

12.7 K from $x = 0.00$ to 0.03 in steps of 0.01 at.% V. For *series B*, T_C first increases at $x = 0.01$ and then decreases with increasing V substitution.

The DSC patterns for *series A* and *B* are measured (not shown here), and the derived latent heat is listed in Table 1. In the previous, $\text{Mn}_1\text{Fe}_{0.95}\text{P}_{0.593-x}\text{Si}_{0.33}\text{B}_x$ alloys annealed at 1373 K in two-step heat treatment were studied^[9]. Note that, it was found that the alloy corresponding to the composition with $x = 0.00$ in this work is already at the border of the FOMT to the second order magnetic transition (SOMT). Increasing the V substitution from 0.00 to 0.03 results in a strong reduction of the latent heat by 67% from 5.2 to 1.7 J/g for the alloys annealed at 1323 K and by 55% from 6.2 to 2.8 J/g for the alloys annealed at 1373 K (listed in table 1), indicating that the samples transfer more towards the SOMT. As mentioned above, the reduction in latent heat mainly contribute to the increase in dT_C/dB . A smaller latent heat will result in a smaller thermal hysteresis.

A large ΔT_{hys} is usually accompanied with a strong FOMT in the materials families of $\text{Gd}_5(\text{Si,Ge})_4$ ^[25,26], $\text{La}(\text{Fe,Si})_{13}$ ^[21], and Heuslers $\text{NiMn}(\text{In,Ga,Sn})$ ^[27] and $(\text{Mn,Fe})_2(\text{P,Si,B})$ ^[28] alloys. Even though they have a giant MCE, the large ΔT_{hys} limits their application in real devices since it will lower the heat exchanging efficiency dramatically. Materials optimized to be near the critical point between a first and second order transition are promising candidates for applications as they combine a low thermal hysteresis with a considerable GMCE^[9]. Here, we find that ΔT_{hys} can be reduced further by substituting Mn by V in $(\text{Mn,Fe})_2(\text{P,Si,B})$ alloys. ΔT_{hys-MT} is determined by calculating the difference in the maximum value of $-dM/dT$ during cooling and heating in an applied magnetic field of $\mu_0 H = 1$ T. For *series A*, ΔT_{hys-MT} decreases by 36% from 1.1 to 0.7 K when x increases from 0.00 to 0.03.

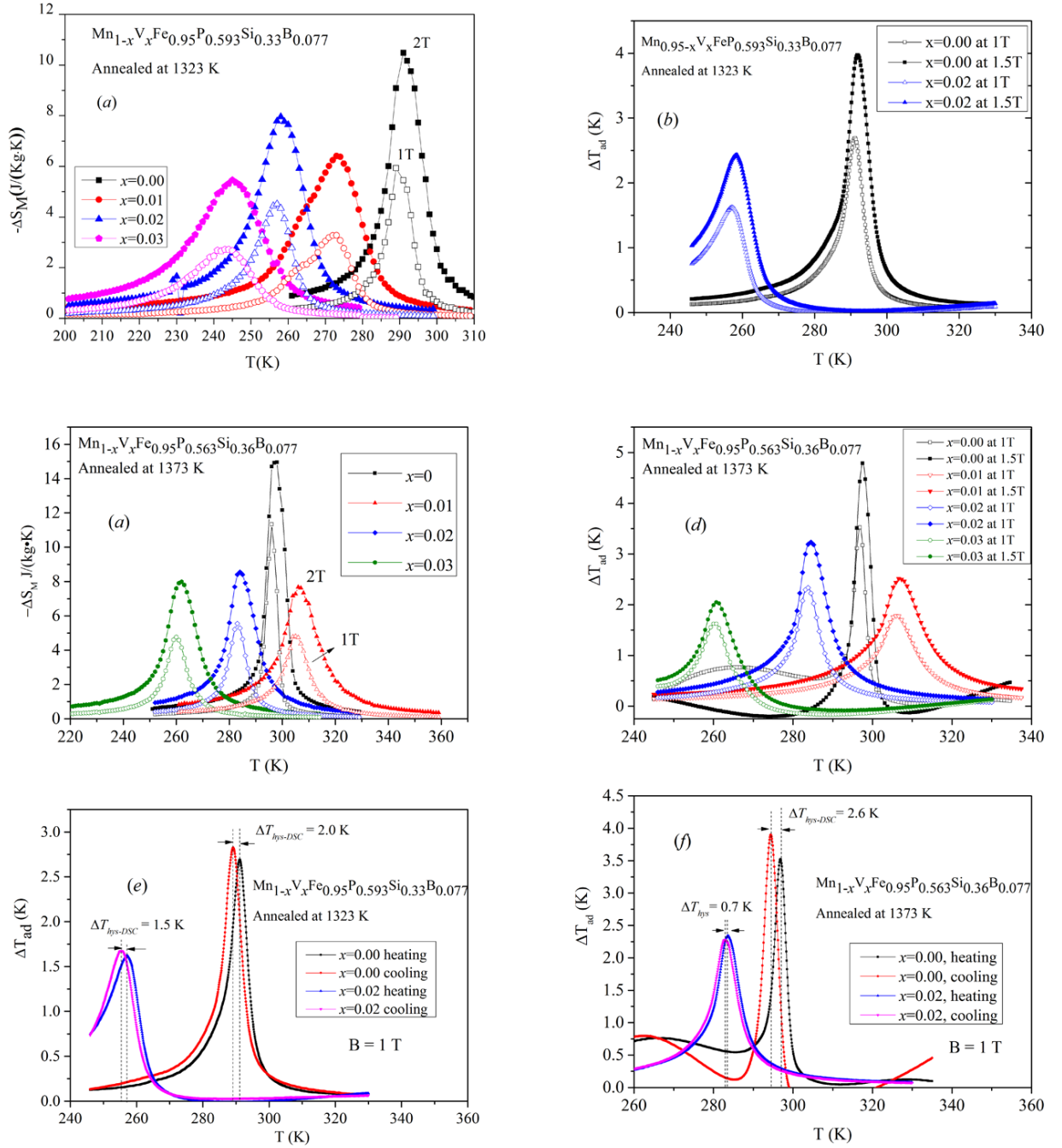


Fig. 3 (a) and (c) Temperature dependence of $|\Delta S_M|$ under a field change of 0-1.0 T (open symbols) and 0-2.0 T (filled symbols) for *series A* and *B*, respectively; (b) and (d) Temperature dependence of ΔT_{ad} under a field change of 0-1.0 T (open symbols) and 0-1.5 T (filled symbols) for *series A* and *B*, respectively; (e) Partial temperature dependence of ΔT_{ad} under a field change of 0-1.0 T during heating and cooling for *series A*; (f) Partial temperature dependence of ΔT_{ad} under a field change of 0-1.0 T during heating and cooling for *series B*.

For *series B*, ΔT_{hys-MT} decreases by 93% from 1.5 to 0.1 K when x increases from 0.00 to 0.03. The thermal hysteresis decreases with increasing V substitution, which tunes the *series A* and *B* alloys towards a second order magnetic transition which makes these materials more suitable for commercialization of magnetic refrigerators.

The iso-field magnetization curves (not shown here) of *series A* and *B* for a magnetic field change of 0-2 T are measured in the vicinity of T_C with a temperature interval of 1 K. The values of $|\Delta S_M|$ for the alloys is derived from extracted isothermal magnetization curves using the Maxwell relation^[29, 30]. The temperature dependence of $|\Delta S_M|$ for *series A* and *B* are shown in figure 3 (a) and (c), respectively. $|\Delta S_M|$ decreases with increasing V substitution. However, the alloy with $x = 0.02$ in *series A* has a higher $|\Delta S_M|$ value even though it has a lower latent heat. In *series A*, the MCE ($|\Delta S_M| = 6.5$ J/(kgK) at 289 K under a field change of 0-1 T with $\Delta T_{hys} = 1.1$ K) of the alloy with $x = 0.00$ is comparable to the previously studied one^[9] prepared by a second step annealing method ($|\Delta S_M| = 9.2$ J/(kgK) at 279.1 K under a field change of 0-1 T with $\Delta T_{hys} = 1.6$ K).

Figure 3 (b) illustrates the temperature dependence of in-field DSC values of ΔT_{ad} for a partial *series A* ($x = 0.00$ and 0.02), while figure 3 (d) illustrates the temperature dependence of ΔT_{ad} for *series A* ($x = 0.00, 0.01, 0.02$ and 0.03). When x increases from 0.00 to 0.02 in *series A*, the value of ΔT_{ad} decreases from 2.7 to 1.6 K under a field change of 1 T. When x increases from 0.00 to 0.02 in *series B*, the values of ΔT_{ad} decreases from 3.5 to 2.3 K under a field change of 1 T. Note that, in *series B*, the value of $\Delta T_{hys-DSC}$, determined by the difference of the heating and cooling process of in-field DSC under a field change of 1 T, decreases from 2.4 to 0.7 K when x increases from 0.00 to 0.02. The value of ΔT_{ad} for $Mn_{0.98}V_{0.02}Fe_{0.95}P_{0.563}Si_{0.36}B_{0.077}$ ($\Delta T_{ad} = 2.3$ K) in *series B* is competitive to the

MnFe_{0.95}P_{0.563}Si_{0.36}B_{0.077} alloys ($\Delta T_{ad} = 2.5$ K) ^[9], but its value of $\Delta T_{hys-DSC}$ is reduced by 85%. In addition, for the *series B*, the latent heat calculated from the calorimetry measurement (which is not shown here) is 5.1 ± 0.02 and 3.3 ± 0.02 J/g for $x=0.00$ and $x= 0.02$, respectively. It is clearly promising to achieve at the same time a giant value of ΔT_{ad} and an extremely low $\Delta T_{hys-DSC}$, which can significantly improve the heat exchange efficiency of the magnetic cooling system.

The magnetic field dependence of T_C and dT_C/dB for *series A* and *B* are shown in figure 4 (a) and (b). The magnetic field (on the horizontal axis) has been corrected by the demagnetizing field using a demagnetization factor of 1/3, as the shape of measuring powders can be simplified as spheres. In order to demonstrate the change in dT_C/dB , the value of $T_C(B)-T_C(0)$ versus the magnetic field is shown in figure 4 (a) and (b). The Clausius–Clapeyron relation for a FOMT corresponds to $dT_C/dB = -T_C\Delta M/L$, where B is the applied magnetic field and ΔM is the jump in magnetization, implying that dT_C/dB should increase with an increase of ΔM and a decrease of the latent heat ^[Error! Bookmark not defined.]. For the alloys annealed at 1323 and 1373 K, dT_C/dB can be enhanced from 4.0 to 5.0 K/T when the V content is changed from $x = 0.00$ to $x = 0.02$. A value of 5.0 K/T is comparable to the dT_C/dB value of (Mn,Fe)₂(P,As) alloys, where dT_C/dB was found to be 5.2 K/T. ^[31] This increase is mainly caused by the decrease of the latent heat (see table 1) since the values of T_C and ΔM are reduced (see Figure 3). Moreover, figure 4 (c) demonstrates that the magnetic moment per formula unit ($\mu_{f.u.}$) for *series B* increases from 3.75 to 3.96 $\mu_B/f.u.$ when x increases from 0.00 to 0.02. The value of $\mu_{f.u.}$ for *series B* was calculated as mentioned in reference [32]. A larger value of $\mu_{f.u.}$ suggests a larger value of $|\Delta S_M|$. The higher values for dT_C/dB and $\mu_{f.u.}$ explains why a ultra-low thermal hysteresis and a giant GMEC can be achieved simultaneously in the alloys with V. By B substitution, the thermal hysteresis reaches a minimum, while ΔT_{ad} remains 2 K.

Introducing V as a new substitutional element is found to be capable of increasing both dT_C/dB and $\mu_{f.u.}$ and can further decrease the hysteresis without losing the GMCE. Thus, the current $Mn_{1-x}V_xFe(P,Si,B)$ compounds provide a feasible alternative for high-frequency near room temperature magnetic cooling applications.

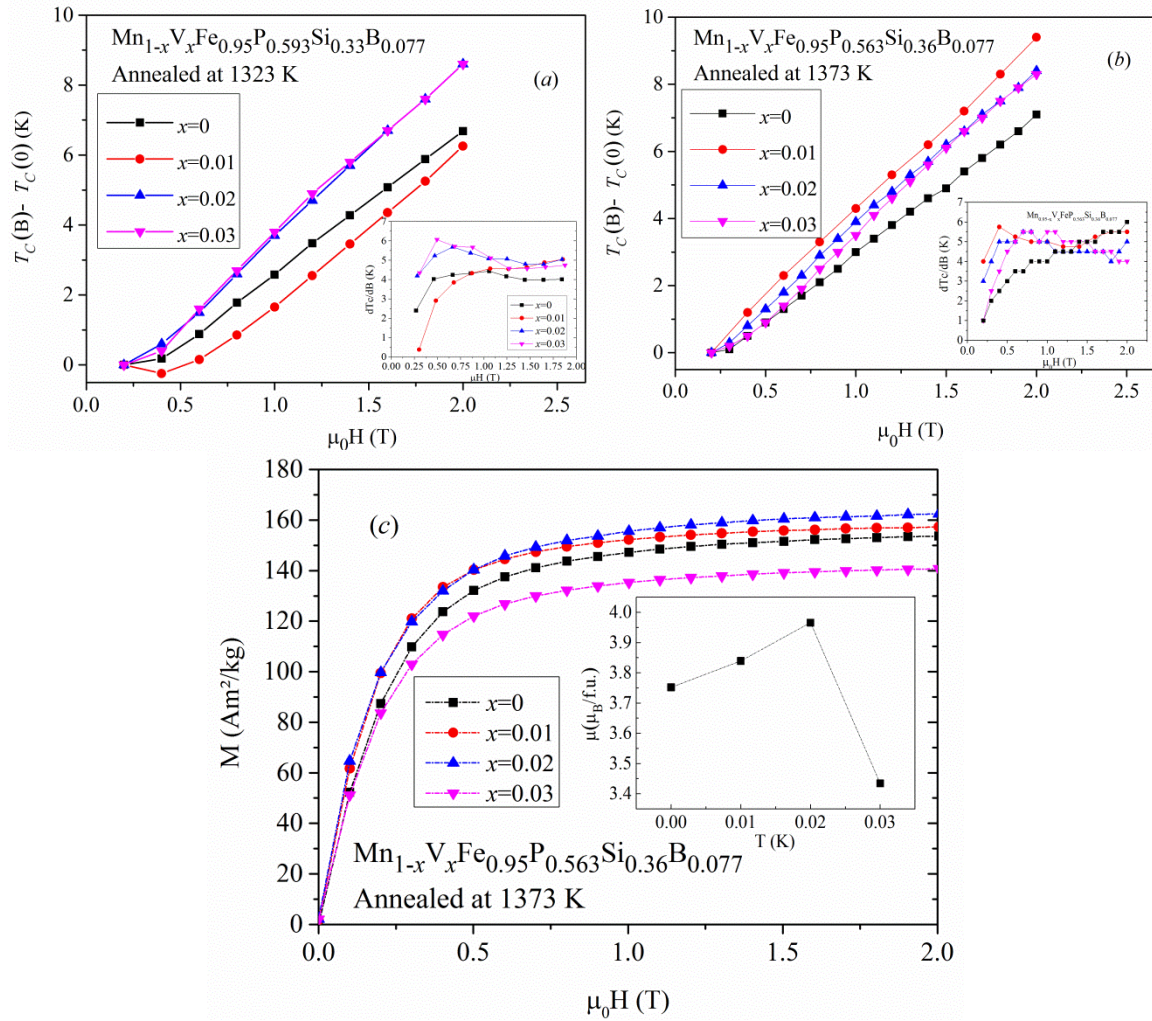


Fig. 4 Field dependence of T_C and dT_C/dB (insets) for *series A* (a) and *series B* (b); (c) The magnetization as a function of the V content for *series A* measured at a temperature of 5 K. The insets are the magnetic moment per formula unit ($\mu_{f.u.}$) dependence of the V content for *series B*.

4. Conclusions

The ultra-low hysteresis and giant MCE of $\text{Mn}_{1-x}\text{V}_x\text{Fe}_{0.95}\text{P}_{0.563}\text{Si}_{0.36}\text{B}_{0.077}$ alloys annealed at 1373 K paves a path to high frequency magnetic refrigeration applications. T_C tends to decrease with increasing V. For the alloys annealed at 1373 K, the latent heat can be reduced by 55 % from 6.2 to 2.8 J/g and $\Delta T_{\text{hys-MT}}$ decreases by 93% from 1.5 to 0.1 K when x increases from 0.00 to 0.03. The field dependence of the transition temperature (dT_C/dB) is enhanced from 4.0 to 5.0 K/T by V substitution of Mn. Higher values of dT_C/dB and $\mu_{\text{f.u.}}$ value are the key reasons that a large GMCE value can be provided even though hysteresis has been reduced to ultra-low values. Finally, an ultra-low value of $\Delta T_{\text{hys-DSC}}$ (0.7 K) and a giant ΔT_{ad} (2.3 K) can be achieved in a field of 1 T. Thus, the current $\text{Mn}_{1-x}\text{V}_x\text{Fe}(\text{P},\text{Si},\text{B})$ compounds can provide a feasible alternative for high-frequency near-room temperature magnetic cooling applications using permanent magnets.

Acknowledgements

The authors acknowledge Anton Lefering, Kees Goubitz and Bert Zwart for their technical assistance. The authors also thank Yibole Hargen for discussion. This work is part of the Industrial Partnership Program IPP I28 of the Dutch Foundation for Fundamental Research on Matter (FOM), financially supported by BASF New Business. This work is also supported by Guangdong Provincial Science and Technology Program (Grant No. 2015A050502015), the Guangzhou Municipal Science and Technology Program (No. 201505041702137), Natural Science Foundation of the Guangdong Province (2016A030313494), and Zhongshan Municipal Science and Technology Program (Platform construction and innovation team). The author thanks for the financial support of the Guangzhou Ethics Project.

References

- [1] E. Brück, O. Tegus, D.T.C. Thanh, K.H.J. Buschow. *Journal of Magnetism and Magnetic Materials*, 310 (2007) 2793-2799.
- [2] V. K. Pecharsky, K. A. Gschneidner. *Physical Review Letters*, 23 (1997) 4494-4497.
- [3] F. X. Hu, B. G. Shen, J. R. Sun, and Z. H. Cheng. *Applied Physics Letters*, 23 (2001) 3675-3677.
- [4] S. Fujieda, A. Fujita, K. Fukamichi. *Applied Physics Letters*, 81 (2002) 1276-1278.
- [5] J. Liu, M. Krautz, K. Skokov, T. G. Woodcock, O. Gutfleisch. *Acta Materialia*, 9 (2011) 3602-3611.
- [6] O. Tegus, E. Brück, K. H. J. Buschow, and F. R. de Boer. *Nature (London)*, 415 (2002) 150-152.
- [7] N. H. Dung, Z. Q. Ou, L. Caron, L. Zhang, D. T. Cam Thanh, K. H. J. Buschow, E. Brück. *Advanced Energy Materials*, 6 (2011) 1215-1219.
- [8] N. H. Dung, L. Zhang, Z. Q. Ou, K.H.J. Buschow. *Scripta Materialia*, 12 (2012) 975-978.
- [9] F. Guillou, G. Porcari, H. Yibole, N. H. van Dijk, and E. Brück. *Advanced Materials*, 17 (2014) 2671-2675.
- [10] N. Trung, L. Zhang, L. Caron, K. Buschow, and E. Brück, *Appl. Phys. Lett.* 96 (2010) 172504.
- [11] J. Liu, T. Gottschall, K.P. Skokov, J.D. Moore, and O. Gutfleisch, *Nat. Mater.* 11 (2012) 620.
- [12] O. Gutfleisch, T. Gottschall, M. Fries, D. Benke, I. Radulov, K. P. Skokov, H. Wende, M. Gruner, M. Acet, P. Entel, M. Farle, *Philosophical transactions. Series A, Mathematical, physical, and engineering sciences* (2016) 374.
- [13] F. Guillou, H. Yibole, G. Porcari, L. Zhang, N. H. van Dijk, E. Brück, *Journal of Applied Physics* 116 (2014) 063903.
- [14] J. Lyubina, *Journal of Physics D: Applied Physics* 50 (2017) 053002.
- [15] K. Engelbrecht and C. R. H. Bahl. *J. Appl. Phys.* 108 (2010) 123918
- [16] N. H. Dung, Z. Q. Ou, L. Caron, L. Zhang, D. T. C. Thanh, G. A. de Wijs, R. A. de Groot, K. H. J. Buschow, E. Brück, *Advanced Energy Materials* 1 (6) (2011) 1215-1219.

-
- [17] A. Fujita, S. Fujieda, Y. Hasegawa, K. Fukamichi. *Phys. Rev. B* 67 (2003) 104416.
- [18] Y. Sutou, Y. Imano, N. Koeda, T. Omori, R. Kainuma, K. Ishida, K. Oikawa. *Appl. Phys. Lett.* 85 (2004) 4358–4360.
- [19] S.A. Nikitin, G. Myalikgulyev, A.M. Tishin, M.P. Annaorazov, K.A. A.L. Asatryan, Tyurin. *Phys. Lett. A* 148 (1990) 363–366.
- [20] H. E. Karaca, I. Karaman, B. Basaran, Y. Ren, Y. I. Chumlyakov, H. J. Maier. *Advanced Functional Materials* 19 (7) (2009) 983-998.
- [21] O. Gutfleisch, T. Gottschall, M. Fries, D. Benke, I. Radulov, K. P. Skokov, H. Wende, M. Gruner, M. Acet, P. Entel, M. Farle. *Philosophical transactions. Series A, Mathematical, physical, and engineering sciences* 374 (2016) 2074.
- [22] R. Bjørk, C. R. H. Bahl, A. Smith, N. Pryds. *International Journal of Refrigeration* 33 (3) (2010) 437-448.
- [23] B. F. Yu, Q. Gao, B. Zhang, X. Z. Meng, Z. Chen. *International Journal of Refrigeration* 26 (6) (2003) 622-636.
- [24] Z. G. Zheng, H. Y. Yu, X. C. Zhong, D. C. Zeng, Z.W. Liu. *International Journal of Refrigeration* 32 (1) (2009) 78-86.
- [25] V. Provenzano, A. J. Shapiro, R. D. Shull. *Nature* 429 (6994) (2004) 850-853.
- [26] A. O. Pecharsky, K. A. Gschneidner, V. K. Pecharsky. *Journal of Applied Physics* 93 (8) (2003) 4722-4728.
- [27] V. Basso, C. P. Sasso, K. P. Skokov, O. Gutfleisch, V. V. Khovaylo. *Physical Review B* 85 (1) (2012).
- [28] E. Brück, O. Tegus, D. T. C. Thanh, K. H. J. Buschow. *Journal of Magnetism and Magnetic Materials* 310 (2) (2007) 2793-2799.
- [29] K. A. Gschneidner, Jr., V. K. Pecharsky, A. O. Tsokol, *Rep. Prog. Phys.* 68 (2005) 1479.
- [30] J. S. Blázquez, V. Franco, A. Conde, T. Gottschall, K. P. Skokov, O. Gutfleisch, *Applied Physics Letters* 109 (2016) 122410.

[31] H. Yibole, F. Guillou, L. Zhang, N. H. van Dijk, E. Brück, *Journal of Physics D: Applied Physics*.
47 (2014) 075002.

[32] J. W. Lai, Z. G. Zheng, R. Montemayor, X. C. Zhong, Z. W. Liu, D. C. Zeng, *Journal of
Magnetism and Magnetic Materials* 372 (2014) 86.